

Phonons in thin GaAs quantum wires

Original

Phonons in thin GaAs quantum wires / Rossi, Fausto; Rota, L.; Bungaro, C.; Lugli, P.; Molinari, E.. - In: PHYSICAL REVIEW. B, CONDENSED MATTER. - ISSN 0163-1829. - 47:3(1993), pp. 1695-1698. [10.1103/PhysRevB.47.1695]

Availability:

This version is available at: 11583/2498618 since:

Publisher:

APS

Published

DOI:10.1103/PhysRevB.47.1695

Terms of use:

This article is made available under terms and conditions as specified in the corresponding bibliographic description in the repository

Publisher copyright

(Article begins on next page)

Phonons in thin GaAs quantum wires

F. Rossi and L. Rota

Dipartimento di Fisica, Università di Modena, Via Campi 213/A, I-41100 Modena, Italy

C. Bungaro and P. Lugli

*Dipartimento di Ingegneria Elettronica, Università di Roma "Tor Vergata,"
Via della Ricerca Scientifica, I-00173 Roma, Italy*

E. Molinari

*Dipartimento di Fisica, Università di Modena, Via Campi 213/A, I-41100 Modena, Italy**
and Consiglio Nazionale delle Ricerche, Istituto "O.M. Corbino,"

Via Cassia 1216, I-00189 Roma, Italy

(Received 14 September 1992)

Phonon frequencies and potentials for an array of thin rectangular GaAs wires embedded in AlAs are calculated within a microscopic scheme. The confined and interface character of optical modes are clearly evident from their dispersion and from the spatial profiles. Our results allow us to conclude that macroscopic models based on the dielectric continuum scheme are adequate to describe confined phonon profiles at wave vectors relevant to el-ph scattering, in contrast with approaches based on mechanical boundary conditions, which yield modes with the wrong symmetry sequence. The implications for electron-phonon scattering rates are discussed.

Much of the recent interest in the properties of polar optical phonons in semiconductor nanostructures is prompted by their relevance to the coupling with carriers, which affects the cooling rates of photoexcited electrons on the picosecond time scale as well as transport phenomena at high temperatures.¹ Electron-phonon (el-ph) scattering rates are of course crucially dependent not only on the frequency spectrum of vibrational modes, but also on the symmetry and spatial extension of their dis-

placement profiles. While the latter have been the subject of extensive research and discussion in two-dimensional (2D) systems,² the same is not true for one-dimensional (1D) structures. Here the available microscopic studies^{3,4} focus on frequency dispersions, and no systematic description of spatial mode profiles exists. On the other hand, recent calculations of phonon-confinement effects on electron energy relaxation in quantum wires (QWR's),⁵ based on macroscopic phonon models, repropose the contraposition of competing approaches as in the early stages of the debate on quantum wells (QW's) and superlattices (SL's).⁶

In this paper, we present the results of a microscopic

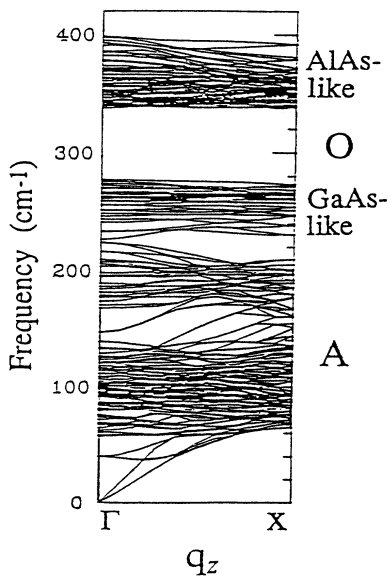


FIG. 1. Phonon dispersion, along the z direction parallel to the wires, for an array of thin rectangular GaAs wires embedded in AlAs (see the text for the detailed wire geometry).

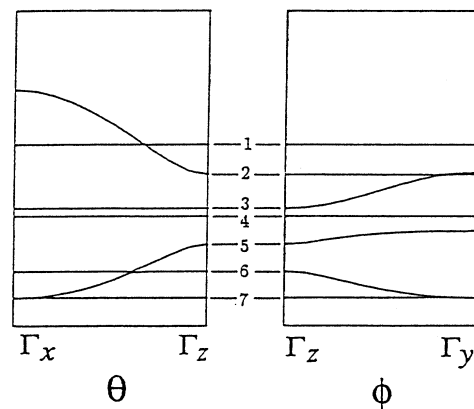


FIG. 2. Angular dispersion of the topmost GaAs-like optical modes at Γ . θ and ϕ are the angles between the direction of the vanishing wave vector and the wire direction, z, in the xz and yz planes, respectively. $\Gamma_x = (q_x \rightarrow 0, 0, 0)$; $\Gamma_y = (0, q_y \rightarrow 0, 0)$; $\Gamma_z = (0, 0, q_z \rightarrow 0)$.

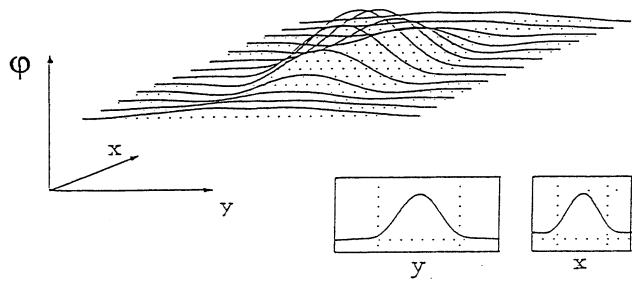


FIG. 3. Potential ϕ of the topmost GaAs-like confined mode (mode 1 of Fig. 2) in the xy plane normal to the wire at $\mathbf{q}=(0,0,q_z=0.15 \text{ \AA}^{-1})$, as calculated from the microscopic phonon displacements. The horizontal dotted lines indicate the zero of the potential. The interface positions are indicated by the vertical dotted lines in the two insets, which show the potential profiles in the planes cutting through the center of the wires.

calculation of phonon frequencies and potentials in thin rectangular GaAs QWR's embedded in AlAs, demonstrating that, for wave vectors along the wire direction, the symmetry of confined optical modes is consistent with the predictions of the dielectric continuum model (DCM).⁷ For "interface modes," the picture we find is much more complex than assumed by simplified models of rectangular wires, based on decoupling between the two directions perpendicular to the wire.⁷ For a correct description of individual phonon profiles, which will be relevant for the interpretation of Raman-scattering experiments, full calculations are therefore needed.

Our microscopic calculations are performed for a periodic array of infinite (100)-oriented GaAs wires of rectangular section, 3 and 5 monolayers (ML) wide along the x and y directions, respectively ($\sim 8.5 \times 14 \text{ \AA}$). The width of the AlAs barrier along x and y is also 3 and 5 ML. The three-dimensional unit cell thus contains 120 atoms. Phonon frequencies and displacements are obtained by direct diagonalization of the dynamical matrix, constructed from *ab initio* interatomic force constants.^{2,8} The important quantity for el-ph interaction is the electrostatic potential $\phi_\nu(q_z; x, y)$ generated by the displacement pattern associated to each phonon mode ν at given wave vector $\mathbf{q}=(0,0,q_z)$. This is calculated from the microscopic displacements⁹ as done in Ref. 2 for QW's. For electrons confined in QWR's, the phonons contributing to el-ph scattering have the wave vector parallel to the wire direction z . We thus plot the full phonon dispersion $\omega=\omega(q_z)$ in Fig. 1. We recognize the acoustical (A) region (up to $\omega \sim 220 \text{ cm}^{-1}$), and the region of GaAs-like and AlAs-like optical (O) vibrations. In the following we focus on the latter.

The angular dispersion of the topmost GaAs-like optical modes at $\mathbf{q} \rightarrow 0$ is displayed in Fig. 2. Here θ and ϕ are the angles between the phonon wave vector and the z direction in the xz and yz planes, respectively. As in 2D systems, some of the modes are found to be dispersive with θ or ϕ ; this is due to the long-range Coulomb interaction, which is indeed anisotropic at Γ .²⁻⁴

In order to discuss the spatial profile and symmetry of confined modes at wave vectors relevant to the el-ph

scattering, in Figs. 3 and 4 we plot the potentials of modes 1 and 4 (dispersionless with θ and ϕ) in the xy plane normal to the wire at $\mathbf{q}=(0,0,q_z=0.15 \text{ \AA}^{-1})$. In spite of the small width of the AlAs barriers, the potentials are well confined within the GaAs region, in full analogy with the behavior of the corresponding thin SL's in 2D.⁹ Clearly, their potential profiles can be factorized in two decoupled confined functions of x and y . For the topmost mode (Fig. 3) both components have even symmetry with respect to the center of the wire, while the potential associated to mode 4 is even along x and odd along y . This symmetry is obviously not compatible with the prediction of the guided-mode model^{6(a)}—according to which the topmost confined mode has a nodeless displacement profile (hence an odd potential with respect to the center of the wire) along x or along y —but fully agrees with the results of the DCM.⁷ A more accurate analytic form of these confined profiles has been proposed by Zhu in Ref. 4.

As the guided-mode model does not satisfy electrostatic boundary conditions at the interfaces, its failure in describing the order of confined modes at wave vectors \mathbf{q} parallel to the wire direction is not surprising. Indeed, the reason why a nodeless-displacement mode is not

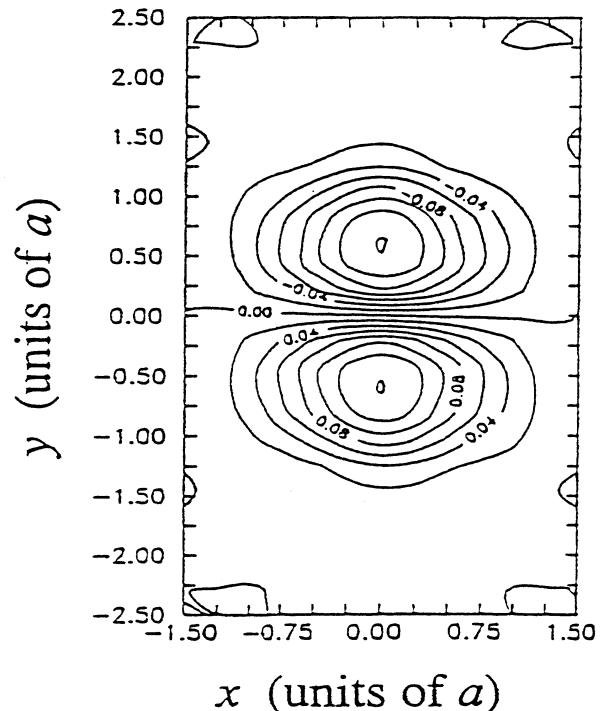


FIG. 4. Equipotential contours (arbitrary units) for the GaAs-like confined mode number 4 (dispersionless in Fig. 2) in the xy unit cell normal to the wire, at $\mathbf{q}=(0,0,q_z=0.15 \text{ \AA}^{-1})$, as calculated from the microscopic phonon displacements. The x and y values are in units of a , the bulk lattice parameter. The wire, 3 and 5 ML wide along the x and y directions, respectively, is centered at $(x,y)=(0,0)$; thus, the four interface As planes are at $x=\pm 0.75a$ and $y=\pm 1.25a$.

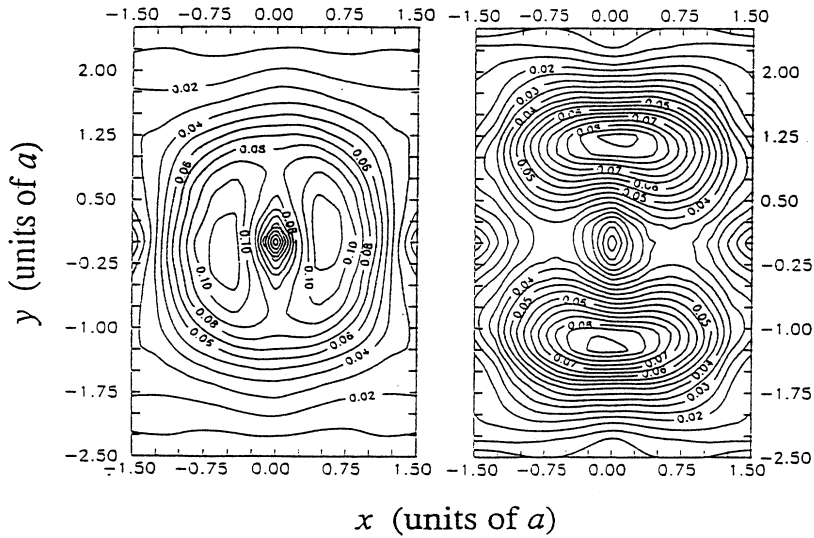


FIG. 5. Contour plots (arbitrary units) of $|\varphi|$ for two GaAs-like modes with interface character (left: mode 2, and right: mode 6 of Fig. 2) in the xy plane normal to the wire, at $\mathbf{q}=(0,0,q_z=0.15 \text{ \AA}^{-1})$, as calculated from the microscopic phonon displacements. Notations as in Fig. 4.

found as the highest-frequency mode at those \mathbf{q} 's is precisely that such modes are the most sensitive to the macroscopic field, which is anisotropic because of the boundary conditions. When the z component of the wave vector increases, their frequency decreases, thereby yielding a mode sequence inconsistent with the guided-mode model, in full analogy with what happens in the 2D case.² The potential of the dispersive modes becomes increasingly localized close to the interfaces with increasing q_z : the angular dispersion thus reflects the “interface character” of the modes.

The moduli of potential profiles for two of the dispersive modes (mode 2 and 6) are displayed in Fig. 5 in the form of contour plots. Consistent with their angular dispersion (non-negligible along θ or ϕ), these modes have maxima only along one pair of interfaces. This is, however, inconsistent with the predictions of simplified versions of the dielectric continuum model,⁷ according to which confined or interface modes exist, the latter having interface character with the same parity in both x and y

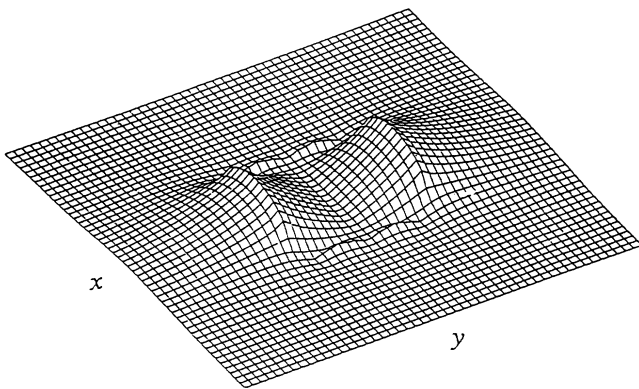


FIG. 6. Potential $|\varphi|$ in the xy plane normal to the wire for one of the modes calculated by numerical solution of the full DCM model (see the text). $\mathbf{q}=(0,0,q_z=0.15 \text{ \AA}^{-1})$.

directions (both even or both odd). Besides the choice of electrostatic boundary conditions, the main assumption of this simplified DCM is the factorization of the phonon potential profile along x and y , which allows us to obtain analytical solutions. Following Knipp and Reinecke¹⁰ we have removed such an assumption by solving the Laplace equation numerically for our wire geometry, with the appropriate boundary conditions. We obtain markedly different results with respect to the simplified model not only for dispersions¹⁰ but also for the spatial profiles of interface modes. In particular, modes with opposite parity along x and y do exist (Fig. 6), and some phonon potentials seem to be compatible with the microscopic findings of Fig. 5. However, for our thin-wire array we could not trace a full correspondence of these modes with the microscopic ones. Further microscopic calculations for larger wires with larger barriers are needed in order to be conclusive on the general ability of the DCM macroscopic description to reproduce not only confined modes but also interface modes of quantum wires.¹¹

Before concluding, we mention the implications of our results for el-ph coupling. For large wires, where the contribution of interface modes is negligible, we expect the DCM description of phonons (in the slab⁷ or Zhu⁴ versions) to provide a good approximation to el-ph *total* scattering rates. These are in turn close to the values obtained for scattering with bulk modes,^{12–16} as expected from our knowledge of 2D systems² and from the validity of the el-ph scattering sum rule.^{17,2,18} The alternative (“guided”) model—whose results were shown to differ significantly from the above picture, yielding a large reduction in scattering rates with respect to the bulk⁵—is thus once more inadequate. For thin wires, our calculations indicate that interface modes must play an important role in el-ph coupling. A detailed calculation of scattering rates is under way.

In summary, we have evaluated phonon frequencies and potentials for an array of thin rectangular GaAs wires embedded in an AlAs matrix. Our results allow us

to conclude that macroscopic phonon models with electrostatic boundary conditions are adequate to describe confined phonon profiles at wave vectors relevant to el-ph scattering, in contrast with mechanical boundary conditions which yield modes with the wrong symmetry sequence. This implies that no major decrease in total el-ph rates must be expected owing to phonon confinement. Important effects on el-ph coupling may then come only

from “geometrical” effects in appropriate wire structures as proposed by Sakaki.¹⁹

This work was supported in part by CNR, Progetto Finalizzato “Calcolo parallelo” (Grant No. 92.01598.PF69), by Consorzio Nazionale Fisica della Materia (INFM), and by the EEC Commission under the Esprit Basic Science project “NANOPT.”

*Present and permanent address.

¹For introductory reviews on quantum wires, see *Nanostructure Physics and Fabrication*, edited by M. A. Reed and P. Kirk (Academic, Boston, 1989).

²H. Rucker, E. Molinari, and P. Lugli, *Phys. Rev. B* **44**, 3643 (1991); **45**, 6747 (1992), and references therein.

³Shang-Fen Ren and Yia-Chung Chang, *Phys. Rev. B* **43**, 11 857 (1991).

⁴Bang-Fen Zhu, *Phys. Rev. B* **44**, 1926 (1991).

⁵V. B. Campos, S. Das Sarma, and M. A. Strosio, *Phys. Rev. B* **46**, 3849 (1992).

⁶These competing models have been used, with contrasting results, also in calculations for cylindrical wires. (a) “Guided mode model”: N.C. Constantinou and B. K. Ridley, *Phys. Rev. B* **41**, 10 627 (1992), and references therein. (b) “Slab mode model”: P. Selbmann and R. Enderlein, *Superlatt. Microstruct.* **12**, 219 (1992).

⁷M. Strosio, *Phys. Rev. B* **40**, 6428 (1989); K. W. Kim, M. A. Strosio, A. Bhatt, R. Michevicius, and V. V. Mitin, *J. Appl. Phys.* **70**, 319 (1991).

⁸E. Molinari, S. Baroni, P. Giannozzi, and S. de Gironcoli, *Phys. Rev. B* **45**, 4280 (1992).

⁹C. Bungaro, P. Lugli, F. Rossi, L. Rota, and E. Molinari, in *Ultrafast Laser Probe Phenomena in Semiconductors and Super-*

conductors, edited by R. R. Alfano [SPE Proc. **1677**, 55 (1992)].

¹⁰P. A. Knipp and T. L. Reinecke, *Phys. Rev. B* **45**, 9091 (1992).

¹¹More detailed results for interface modes will be presented elsewhere: E. Molinari, C. Bungaro, F. Rossi, L. Rota, and P. Lugli, in *Phonons in Semiconductor Nanostructures*, edited by J. P. Leburton, J. Pascual, and C. M. Sotomayor Torres (Plenum, New York, in press); (unpublished).

¹²V. B. Campos and S. Das Sarma, *Phys. Rev. B* **45**, 3898 (1992).

¹³V. Bockelmann and G. Bastard, *Phys. Rev. B* **42**, 8947 (1990).

¹⁴S. Briggs and J. P. Leburton, *Phys. Rev. B* **38**, 8163 (1988); D. Jovanovic, S. Briggs, and J. P. Leburton, *ibid.* **42**, 11 108 (1990); S. Briggs and J. P. Leburton, *ibid.* **43**, 4785 (1991); J. P. Leburton, *ibid.* **45**, 11 022 (1992).

¹⁵N. Mori, H. Momose, and C. Hamaguchi, *Phys. Rev. B* **45**, 4536 (1992).

¹⁶L. Rota, F. Rossi, P. Lugli, E. Molinari, S. M. Goodnick, and W. Porod, in *Advanced Semiconductor Epitaxial Growth Processes and Lateral and Vertical Fabrication*, edited by R. J. Malik *et al.* [SPE Proc. **1676**, 161 (1992)]; P. Lugli, L. Rota, and F. Rossi, *Phys. Status Solidi B* **173**, 229 (1992).

¹⁷N. Mori and T. Ando, *Phys. Rev. B* **40**, 6175 (1989).

¹⁸L. F. Register, *Phys. Rev. B* **45**, 8756 (1992).

¹⁹H. Sakaki, *Jpn. J. Appl. Phys.* **28**, L314 (1989).